

PG-LSTM: A Hybrid Model Addressing Spatiotemporal Dependencies for Forecasting of Short-Term Traffic Volume

Chunling Ding*

College of Computing and Information Technologies, National University
Manila 1008, Philippines
School of Big Data and Artificial Intelligence, Anhui Xinhua University
Hefei 230088, P. R. China
chlding@126.com

Roben A. Juanatas

College of Computing and Information Technologies, National University
Manila 1008, Philippines
rajuanatas@national-u.edu.ph

Mideth Abisado

College of Computing and Information Technologies, National University
Manila 1008, Philippines
mbabisado@national-u.edu.ph

*Corresponding author: Chunling Ding

Received April 27, 2025, revised May 23, 2025, accepted May 24, 2025.

ABSTRACT. *The high complexity and dynamics of urban transportation make the spatial and temporal dependence of traffic volume difficult to be captured effectively, which make the accurate prediction of traffic flow a major challenge. This paper analyzes the temporal-spatial features of traffic volume from different perspectives, by combining the historical temporal correlation and road network spatial correlation in traffic volume data, develops a hybrid model named PG-LSTM for short-term traffic volume forecasting which integrates Pearson correlation analysis (PCC) for spatial feature selection, graph convolutional networks (GCN) for spatial dependency modeling, and LSTM for temporal dependency modeling. The PCC method is used to identify road segments in the network that have strong correlations to the traffic volume of the target segment. Considering the road networks' graph-like properties, GCN is employed to capture spatial dependencies in the traffic volume of road segments. By integrating LSTM with GCN, the proposed PG-LSTM model synergistically integrates GCN's spatial modeling capability with LSTM's temporal dynamics learning capability, and enables precise traffic volume forecasting for target road segments. Using the real traffic volume data taken from PeMS system in California, USA, comparison experiments are conducted to evaluate PG-LSTM against other four models (CNN-LSTM, LSTM, GRU, BP) across multiple indicators - including Mean Absolute Error (MAE), Root Mean Square Error (RMSE), Mean Absolute Percentage Error (MAPE) and explanatory power metrics (R^2). The experimental results confirm that the proposed PG-LSTM model is significantly better than the other four comparison models in all four evaluation indicators.*

Keywords: GCN Network; Long Short-Term Memory Network; PCC; traffic volume prediction; temporal-spatial features

1. Introduction. With the acceleration of urbanization and population growth, road traffic has become the most critical component of urban transportation systems [1]. To meet the growing demand for transportation, many cities are actively developing and expanding their road networks, including constructing new roads, upgrading existing ones, and adding traffic infrastructure. As transportation networks evolve and traffic demand increases, traffic flow prediction has become increasingly important. Precise traffic flow forecasting can assist traffic management agencies in optimizing signal timing, dynamically adjusting route guidance, and disseminating real-time traffic information. These measures enhance operational efficiency, mitigate congestion, lower emissions, and ultimately promote the sustainable development of urban mobility systems. Improvements in transportation modernization and the rapid development of big data, artificial intelligence, connected vehicle technology and intelligent management technology have made it a reality to access to traffic flow data timely, reasonable and reliable. To maximize the effectiveness of existing transportation infrastructure, many cities have established big data platforms for traffic flow prediction. These platforms analyze traffic flow data to uncover underlying patterns, extract and process traffic information, and ultimately provide enhanced travel services for transportation participants [1]. However, the inherent stochasticity and nonlinear dynamics of traffic flow pose fundamental challenges for prediction accuracy. To address this challenge, researchers worldwide have employed various advanced techniques for traffic flow modeling and forecasting.

Traffic flow forecasting actually refers to predicting information that can reflect traffic conditions. It forecasts the traffic state of a roadway at the next time period based on historical traffic status of the road and applies certain model algorithms. In practical research, the parameters that can reflect the status of traffic primarily encompass traffic volume, vehicle speed, and roadway occupancy rate [2], among others. According to different time horizons of prediction, traffic volume forecasting can be categorized into short-term forecasting and long-term forecasting. Long-term traffic volume forecasting typically utilizes data with larger time intervals, usually exceeding one hour, and covers extended forecasting periods, primarily serving advance planning purposes. In contrast, short-term traffic flow prediction employs much shorter time intervals, generally within 30 minutes and often in multiples of 5 minutes [3], it mainly provides solutions for instant traffic control.

Currently, prediction models for short-term traffic volume mainly include models based on linear theory, nonlinear theory, and intelligent prediction models. Linear theory models assume that traffic flow data is periodic and that historical traffic flow data follows certain statistical patterns, which can be utilized to predict future flow data. Linear-theory-based models predominantly encompass time-series analysis models, the historical mean model, and the Kalman filtering model. The Kalman filter is a linear filtering method proposed by Kalman [4]. This type of model simulates traffic operation through a state space approach and then obtains traffic flow prediction results through recursive state-space estimation. Nonlinear prediction methods primarily include three types of models: nonparametric regression methods, wavelet analysis methods, and chaos theory methods. Z. Liu et al. [5] argued that the reliability of K-NN model results is uncertain and proposed quantifying the uncertainty in traffic flow point predictions by constructing prediction intervals associated with point forecasts, thereby extending the K-NN method. G. K. Shen [6] proposed an enhanced wavelet neural network model refined by the harmony search algorithm (HS-WNN) for short-term traffic volume forecasting, effectively improving its convergence speed. R. Tang et al. [7] conducted a quantitative analysis and identified the chaotic dynamics in traffic flow fluctuations and demonstrating the data's

predictability. Based on these findings, they developed a hybrid GQPSO-WNN prediction model incorporating phase space reconstruction.

With the rapid advancement of big data, artificial intelligence and cloud computing technologies, researchers have proposed many new methods for processing nonlinear feature data, such as support vector regression, neural network and modern deep learning frameworks. These intelligent nonlinear prediction models can achieve more accurate learning outcomes through adaptive learning capabilities. As an emerging intelligent prediction algorithm, deep learning has attracted extensive attention from scholars worldwide. Deep learning-driven intelligent prediction models have dominated the field. Y. Zhang et al. [8] introduced a traffic flow forecasting solution for traffic flow grounded in Deep Belief Networks (DBN), employing genetic algorithms to identify optimal parameters across different time periods. Y. Jin et al. [9] developed an improved stacked autoencoder model using a greedy layer-wise training method, with experimental results demonstrating that the enhanced model outperforms both SVM and DBN models in terms of prediction accuracy. R. Soua et al. [10] developed a framework that integrates data streams (traffic flow, weather conditions) and event data through D-S evidence theory for traffic volume prediction based on DBN.

In recent years, numerous scholars have demonstrated that Recurrent Neural Networks (RNN) outperform other models in handling temporal dependencies. R. Madan et al. [11] employed discrete wavelet transform for data preprocessing, followed by Autoregressive Integrated Moving Average (ARIMA) models and RNNs. Their experimental results conclusively validated RNN's superior performance in time-series forecasting tasks. Y. Kim et al. [12] took the RNN model as the basic framework and combined with traffic network data to create a spatio-temporal graph to acquire the spatiotemporal interaction characteristics of adjacent road sections, and integrating the dynamic evolution law of time series to realize the accurate prediction of traffic speed of multi-road network. W. Zhang et al. [13] argued that existing models cannot fully explore the spatiotemporal features of traffic data, and they developed a CNN-based deep learning framework. Firstly, optimal input parameters including temporal delays and spatial data volume are determined through the spatiotemporal feature selection algorithm (STFSA). The captured spatiotemporal feature data is transformed into a two-dimensional matrix, and then use CNN to learn the features and construct a prediction model. Comparative analysis of the prediction results with real traffic data showed that the proposed model had a higher prediction accuracy. H. Yu et al. [14] proposed a model named SRCN by integrating Deep Convolutional Neural Networks (DCNN) and LSTM networks. In this hybrid architecture, DCNN captures the spatial dependencies, while LSTM learns temporal patterns.

GCN extends convolutional operations to graph-structured data, enabling neural networks to learn feature representations of nodes and their neighbors. GCN has become a popular deep learning model dedicated to processing graph-structured data and is highly favored in traffic flow prediction. Z. R. Ge et al. [15] proposed a hybrid prediction model named WAC-GCN by combining wavelet analysis with two-dimensional convolutional neural network and graph convolutional neural network. This model extracts the spatial correlation features among nodes by constructing the spatial correlation heat map of the nodes, and optimizes the model parameters using the control variable method, and its prediction accuracy is significantly better than that of the benchmark model. H. Zhang et al. [16] used RetNet as the basic framework to process the long sequence information, combined with GCN to extract the spatial correlation of nodes to aggregate the features of traffic intersection nodes, and the constructed hybrid model effectively improves the robustness and accuracy of traffic volume forecasting.

To leverage the advantages of various prediction methods and achieve more optimal forecasting results, multi-model integration has emerged as a research hotspot in the field of traffic flow prediction in recent years. In real-world road networks, traffic conditions are complex and dynamic, with traffic flow variations influenced by various exogenous factors such as holidays and weather conditions, which resulting in strong nonlinearity, randomness, and periodicity in traffic flow data, as well as obvious temporal and spatial correlations. To more effectively capture traffic flow's spatiotemporal characteristics, this study employs Pearson correlation coefficient analysis to identify road segments with strong traffic flow correlations to target road segment within the traffic network. By conceptualizing the traffic network as a graph, we utilize GCN to capture spatial features of traffic flow, integrates LSTM models with GCN architectures to construct a hybrid prediction model, enabling accurate traffic flow forecasting for target road segments.

2. Traffic Volume Features Analysis. Traffic flow refers to the stream of vehicles traveling on roadways, with key macroscopic indicators including traffic volume, density, speed and so on. This study utilizes real traffic flow data from California highways provided by the PeMS (Performance Measurement System) website, which records fields such as date, traffic volume, number of lanes, and average speed. This paper uses traffic volume as a key indicator to uncover spatio-temporal regularities in flow behavior. Nine road segments at an intersection in the Oakland area of California (as shown in Fig. 1) from the PeMS system are used as research objects to reveal traffic volume's spatiotemporal characteristics.

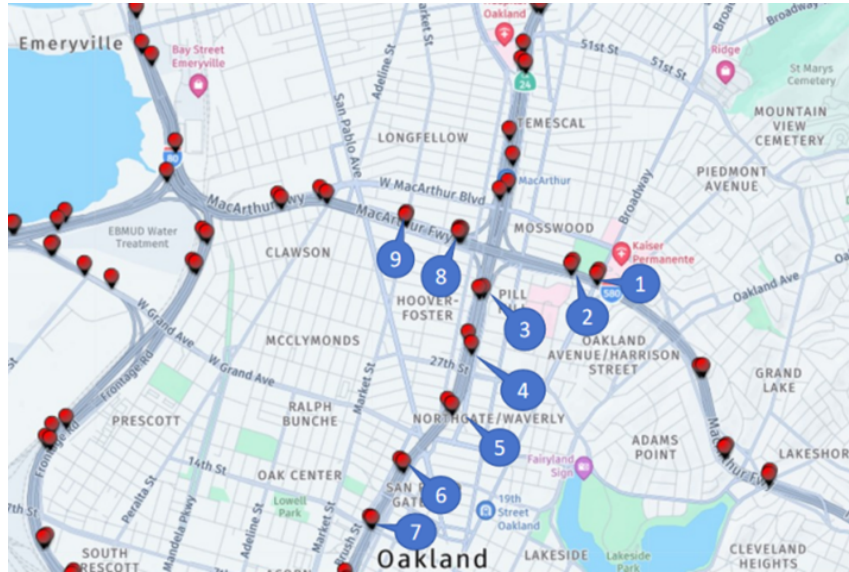


FIGURE 1. Experiment data segment network

2.1. Analysis of Temporal Features. Temporal features analysis plays a core role in traffic prediction, as it can help people gain a deeper understanding of the changing patterns and influencing factors of traffic flow [17]. Traffic flow data has periodicity, and the weekly data changes are similar. Temporal variations of traffic volume, particularly those occurring at weekly and daily scales, exert substantial influence on traffic flow patterns, which deserves special attention. In this study, we select the traffic data at a specific roadway segment from the PeMS system for visualization analysis, showing the periodicity patterns of traffic flow fluctuation at various timescales (daily/weekly).

There is a significant difference in the trend of traffic volume changes between weekdays and weekends. By analyzing the daily traffic volume trends over a week, the patterns of traffic volume changes between workdays and non-workdays can be revealed. Using traffic volume data from a highway segment over a week, a two-dimensional line chart was plotted to display the hourly traffic volume for each day, as shown in Fig. 2. The horizontal axis represents the 24 hours of the day, while the vertical axis represents the aggregated traffic volume every hour. The analysis results indicate that there is a distinct bimodal distribution of traffic volume on weekdays, with prominent surges coinciding with morning and evening commute periods, whereas weekend traffic remains relatively stable. This regular variation provides important insights for traffic volume prediction.

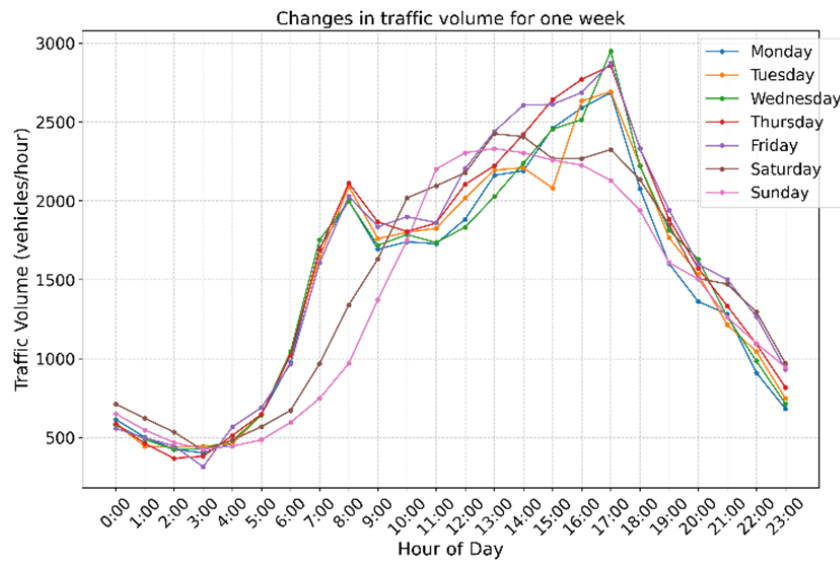


FIGURE 2. Two-dimensional line plot of traffic volume on a section of a highway at different moments of the week

To observe the change tendency of traffic volume at different moments of each day in the week of this road section more clearly, and reveal the temporal dependency patterns between traffic flow at different times and days of the week, the two-dimensional line graph is converted into a three-dimensional image as shown in Fig. 3. From Fig. 3 we can get a clearer picture of the changing patterns of traffic volume, which reflects the different traffic demand and behavioral patterns of weekdays and rest days, and provide a basis for the subsequent traffic volume prediction.

Another focus of temporal feature analysis is intra-day variability, which refers to the trend of traffic volume over the course of a day. By analyzing the features of time-of-day traffic volume variation, such as the peaks of traffic volume in the morning and evening peaks, the temporal distribution pattern of traffic volume during the day can be understood. The intra-day variation is also related to whether it is a weekday or not. Fig. 4 shows the traffic flow changes of a certain road section on Mondays of multiple weeks.

As shown in Fig. 4, on weekdays, the intra-day variation of traffic volume presents a distinctive feature. Typically, there is a significant increase in traffic volume during the morning peak hour (7:00–9:00) and the afternoon peak hour (16:00–18:00). These peak hours are often accompanied by traffic congestion and reduced travel speeds, creating roadway access challenges. However, compared with weekdays, the intra-day variation of traffic volume on non-weekdays shows different characteristics. As shown in Fig. 5.

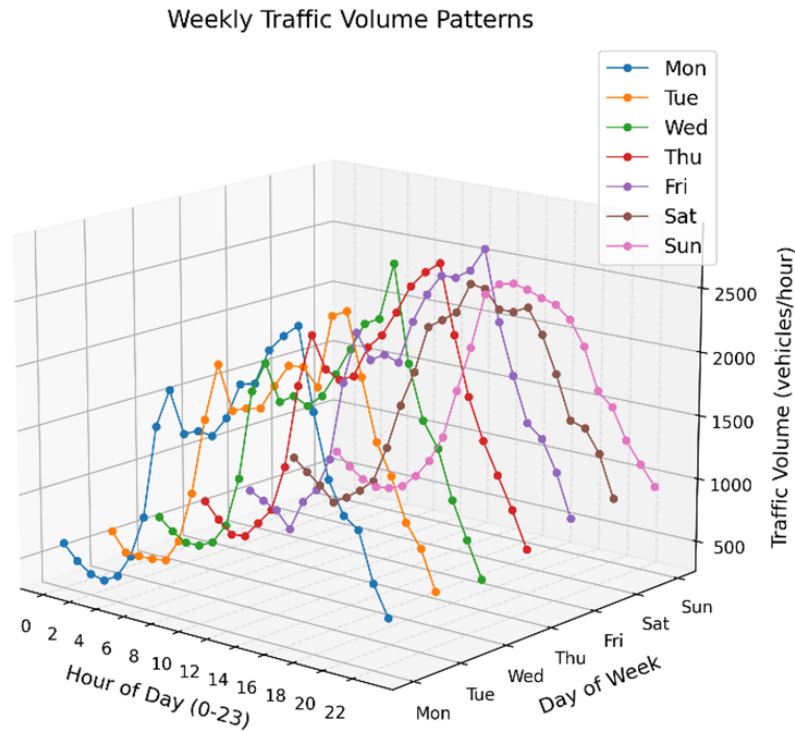


FIGURE 3. Three-dimensional line plot of traffic volume on a section of a highway at different times of the week

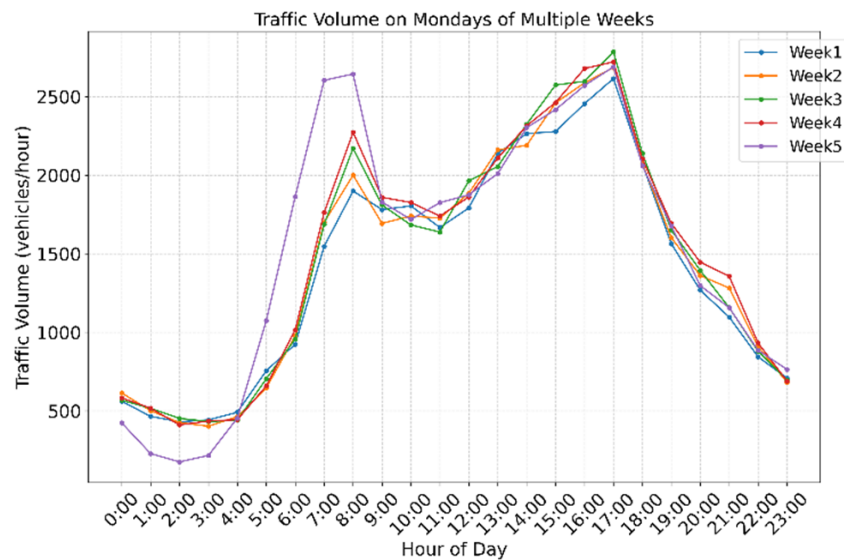


FIGURE 4. Two-dimensional line plot of traffic volume at different times on Mondays of multiple weeks

The daytime traffic volume on non-weekdays is relatively smooth, with only one peak hour that lasts for a long time, from 10 a.m. to 4 p.m. This is because people usually wake up later on rest days, so the peak hour starts relatively late. Because people may go out for pleasure or other leisure activities, people's travel times and purposes are relatively more dispersed and there is no significant concentration of travel demand. By

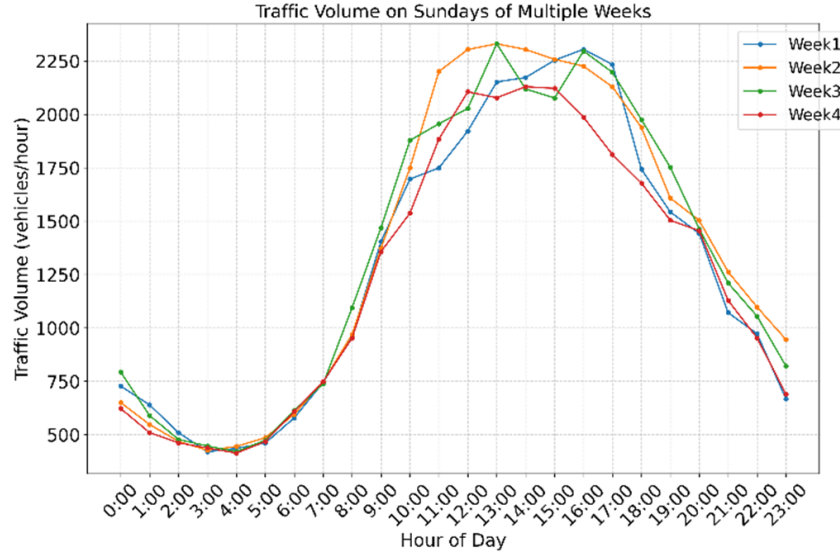


FIGURE 5. Two-dimensional line plot of traffic volume at different times on Sundays of multiple weeks

observing the above four graphs, it can be concluded that the temporal characterization of the weekly and intra-day variations are important for traffic volume prediction. The weekly variation reflects the difference in traffic demand between weekdays and rest days, while the intra-day variation reveals the trend of traffic volume over the course of a day. By analyzing these temporal features in depth, it is possible to predict future changes in traffic flow.

2.2. Analysis of Spatial Features. Spatial features analysis is also a key factor affecting traffic volume prediction [18]. Road network's spatial analysis helps comprehend traffic distribution among different regions. Congestion effects spread through the transportation network, causing adjacent sections to influence each other's traffic conditions and when the traffic volume of a road section is too high, it may have an overflow effect on the traffic volume of adjacent road sections. At the same time, traffic volumes in different regions during the same period of time may also affect each other, and an increase in traffic volume in one region may cause changes of traffic volume in neighboring regions due to traffic demand and spatial continuity of the transportation network.

To further understand the spatial distribution characteristics of traffic volume, we select four adjacent traffic sections 1–4 from the traffic road network (See Fig. 1), obtain their traffic volume data collected on the same day and plot a line graph. Fig. 6 illustrates the traffic volume trends on the same day for these four roadway segments.

By observing Fig. 6, it can be found that the traffic volume trends of the four neighboring road sections are generally similar. Sections 1 and 2 are upstream and downstream sections in the same direction, and their traffic flow change trends are more similar; similarly, sections 3 and 4 are upstream and downstream sections in the same direction, and their change trends are more similar. This indicates that when the traffic volume of one roadway section changes, the traffic volume of the adjacent roadway sections will also change accordingly, showing the influence between adjacent roadway sections.

2.3. Traffic Volume Correlation Analysis. To better illustrate the result of spatiotemporal characteristic analysis of traffic volume, PCC method is adopted to quantitatively analyze the above traffic volume data. In statistics, PCC is a commonly used standard metric for evaluating two variables' correlation, and its value falls between -1

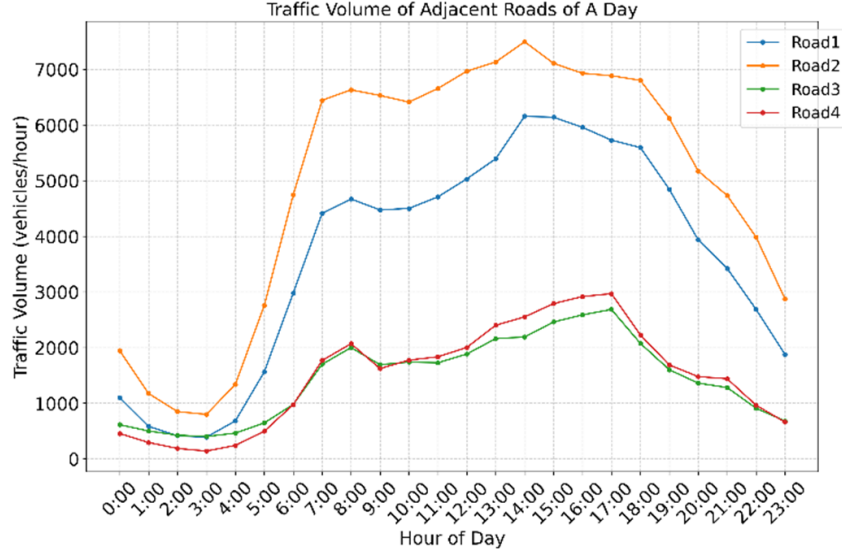


FIGURE 6. Two-dimensional line plot of traffic volume on several adjacent roads at different moments of a day

and 1, which can indicate the direction of the correlation as well as the strength of the correlation [19].

Use $x = \{x_1, x_2, \dots, x_n\}$ and $y = \{y_1, y_2, \dots, y_n\}$ to represent the time-series data of traffic volume, and the correlation coefficient between a and b can be calculated as follows:

$$r(x, y) = \frac{n \sum_{i=1}^n x_i y_i + (\sum_{i=1}^n x_i) (\sum_{i=1}^n y_i)}{\sqrt{n \sum_{i=1}^n x_i^2 - (\sum_{i=1}^n x_i)^2} \sqrt{n \sum_{i=1}^n y_i^2 - (\sum_{i=1}^n y_i)^2}} \quad (1)$$

In (1), (x, y) is a pair of traffic flow sequences for correlation analysis, x_i and y_i are the size of traffic volume at moment i , and n is the length of traffic flow sequence. The closer $r(x, y)$ is to 1, it signifies that x and y are more correlated; and when $r(x, y)$ is less than 0.5, it indicates that the correlation between x and y is low; when $r(x, y)$ equals 0, it signifies that there is no correlation between x and y [20].

Because of the cyclical nature of traffic volume, we selected traffic volume data for a certain road segment from the PeMS dataset for one week (August 8–14, 2022) and conducted correlation analysis on the traffic volume of each day within the week. Figure 7 illustrates the correlation settlement results.

From Figure 7, it can be found that weekday traffic volumes on the same roadway show a strong correlation, with correlation coefficients above 0.94. The correlation between non-weekday traffic volumes on the same roadway is also strong, and the correlation coefficient is 0.94. The difference is that the correlation between traffic flow data between workdays and non-workdays is relatively weak, with correlation coefficients generally below 0.9. This quantitatively illustrates the pattern of traffic flow changes shown earlier through the visualization of line plots.

The Pearson correlation coefficient method is also applicable to traffic network analysis, which can effectively quantify the correlation between traffic volume in different road sections, thus revealing the spatial dependence characteristics of traffic volume. Here, we calculate the correlation between the traffic volume of the 9 road segments marked in Figure 1. The following Figure 8 shows the analysis results.

By observing Figure 8, we can find that the traffic volume correlation between adjacent road segments 1 and 2, which have upstream and downstream relationships, is very strong,

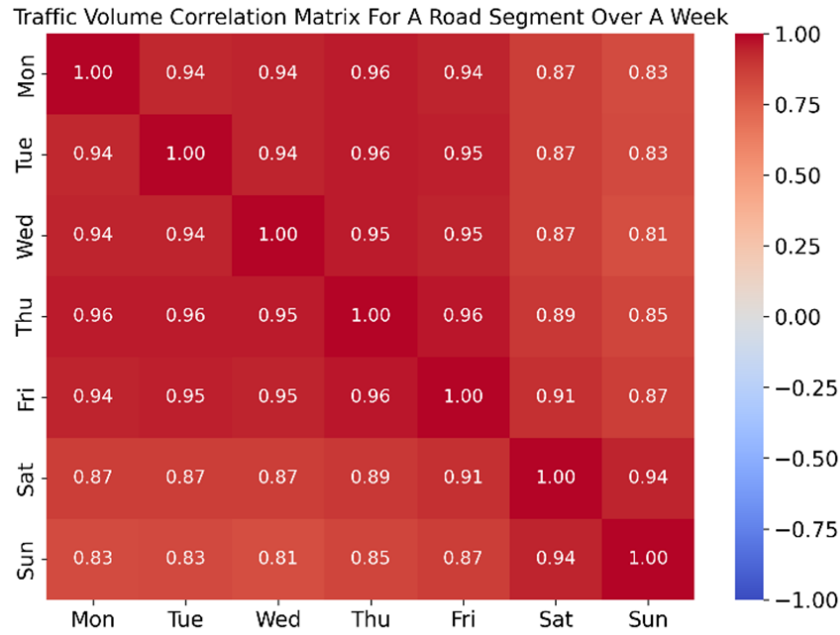


FIGURE 7. Correlation analysis of one week's traffic flow on a road segment

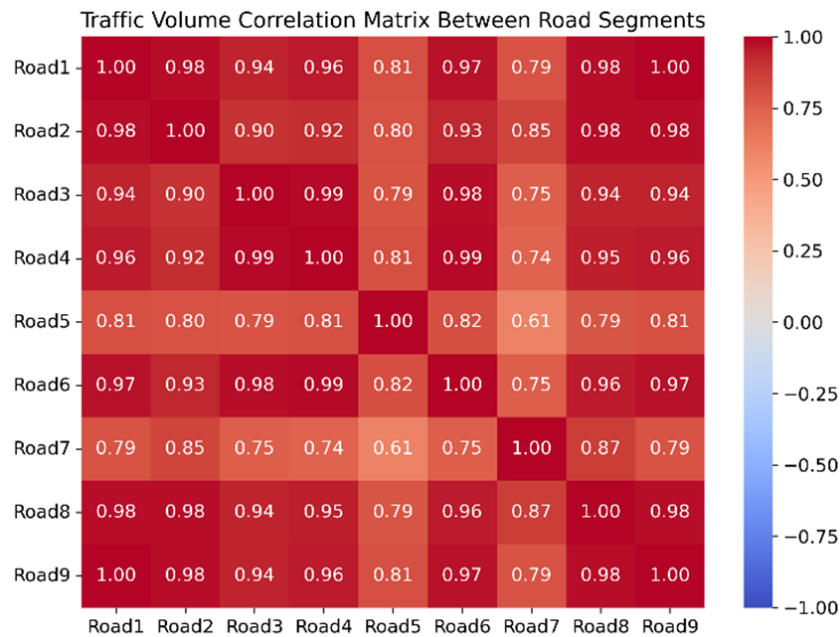


FIGURE 8. Correlation analysis of traffic flow between road segments

with a correlation coefficient of 0.98. And similarly, the correlation between adjacent road segments 3 and 4 is very strong, with a correlation coefficient of 0.99. The correlation between adjacent road segments 8 and 9 is also very strong, with a correlation coefficient of 0.98. Road segments 3 and 6, although they are non-adjacent, also have a strong correlation between their traffic volume, with a correlation coefficient of 0.98.

3. Traffic Volume Prediction Model Building on LSTM. The prediction of traffic volume belongs to the time series prediction problem. RNNs show significant advantages in dealing with time series problems, and LSTM is an improved recurrent neural network,

which not only inherits the advantages of the RNN in time series prediction, but also solves the problem of long-term dependence of RNN [21].

3.1. LSTM Model Structure. LSTM is an enhanced version of the traditional RNN, in the LSTM network structure, the neurons of the RNN are replaced with a special cell structure in the hidden layer part. The cell structure adopts gating mechanism containing three important parts: input gate, output gate, and forgetting gate, to create a controllable memory neuron [22]. The following Figure 9 displays the cell unit's structure of LSTM.

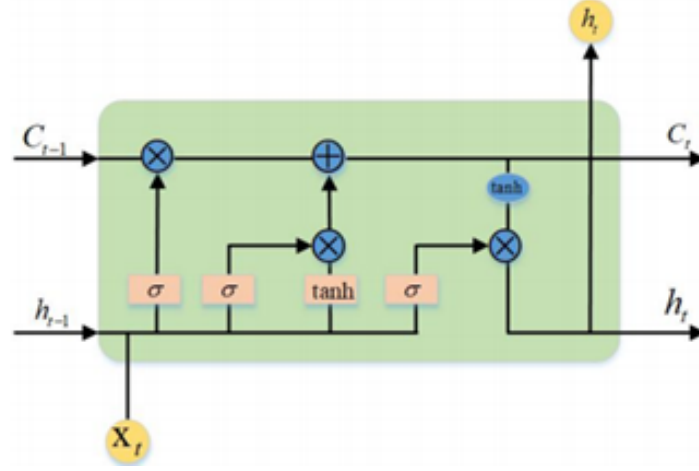


FIGURE 9. Basic unit structure of LSTM

In the LSTM structure, the current neuron has three inputs at current time step t : x_t is external input at the current moment, h_{t-1} is the hidden state output by the LSTM cell at the previous time step, carrying the historical sequence information, and C_{t-1} is the state of the memory cell at the previous moment. The gate structure subtly filters information through a neural layer of sigmoid function and a point-by-point multiplication operation. A probability value between 0 and 1 is generated by the sigmoid layer, indicating the degree of information passage, where 0 means “no information is allowed to pass” and 1 means “all information passes”. The gate structure learns what information to keep or forget during the training process.

3.1.1. Forget Gate. The forget gate is designed to determine the degree of loss of memorized information, and Figure 10 shows its structure. The forget gate takes the current time step input x_t and the previous hidden state h_{t-1} as its inputs, and learns according to (2). The output of this layer f_t is a number between 0 and 1, the value of f_t determines how much of the previous cell state C_{t-1} is forgotten. 1 means that the previous memory cell status information is completely retained, and 0 means that the previous memory cell status information is completely discarded.

$$f_t = \sigma(W_f x_t + U_f h_{t-1} + b_f) \quad (2)$$

In (2), W_f and U_f are the weight matrices mapping the input of the hidden layer at the current moment and the output state of the previous unit to the forget gate; b_f is the threshold offset of forgetting gate, which is the “hidden switch” that regulates long-term memory capacity. σ is the gate activation function, which can be chosen as sigmoid.

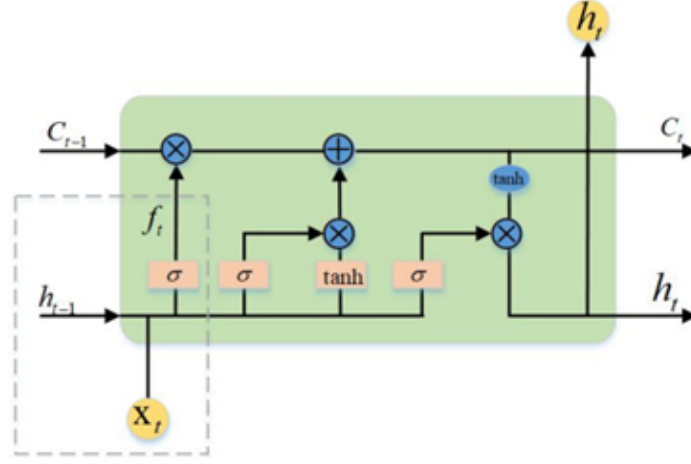


FIGURE 10. Structure of forgetting gate

3.1.2. *Input Gate.* The input gate's role is like a filter, it regulates how much of the current input x_t should be stored into the cell state C_t . Figure 11 shows the structure of input gate.

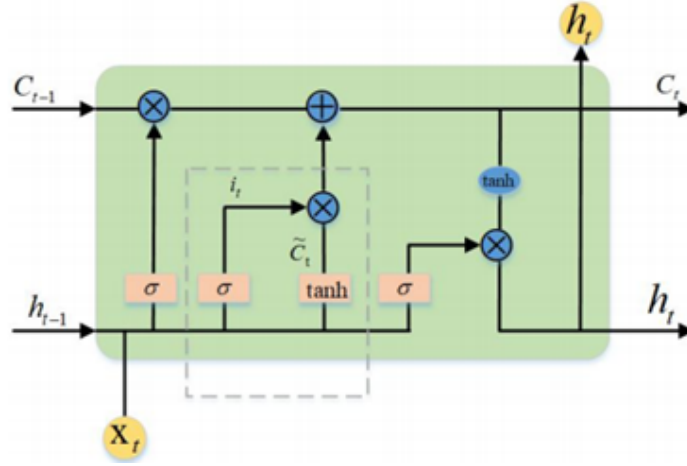


FIGURE 11. Structure of input gate

The amount of new input information injected is jointly regulated by the input gate in concert with the hyperbolic tangent function \tanh . A new state output vector \tilde{C}_t can be obtained by operating the last output with the current new input information through the activation function, and the output i_t of the input gate indicates the rate of adding new information to the current network. i_t and \tilde{C}_t are computed as (3) and (4).

$$i_t = \sigma(W_i x_i + U_i h_{t-1} + b_i) \quad (3)$$

$$\tilde{C}_t = \tanh(W_C x_i + U_C h_{t-1} + b_C) \quad (4)$$

In (3) and (4), W_i and U_i denote the weight matrices and their values are generated by learning through model training, which map x_t and h_{t-1} to the input gate. W_C and U_C denote the weight matrices that map x_t and h_{t-1} to the candidate cell state \tilde{C}_t . b_i is the threshold offset of input gate, it is adaptively adjusted during training and is used to regulate the acceptance of new information, b_c is the threshold offset of candidate memory cell and is used to adjust the distribution of candidate values. σ is the gate activation

function. C_t is the memory cell state at the current moment, it consists of two parts: previous cell state C_{t-1} multiplied with the forget gate f_t by elements, and the candidate state \tilde{C}_t multiplied with i_t by elements. The memory cell state C_t at time step t is gotten by adding the two products. The calculation equation is shown in (5).

$$C_t = f_t \circ C_{t-1} + i_t \circ \tilde{C}_t \quad (5)$$

3.1.3. Output Gate. The output gate determines how much information is needed for the next learning step of the network, and Figure 12 shows the output gate structure. First the ratio of the information output in the cell state o_t is determined by the sigmoid function, as shown in (6). Then the cell state C_t is scaled using the tanh function, and the result is then multiplied element by element with o_t to obtain the output h_t of the current layer, as shown in (7).

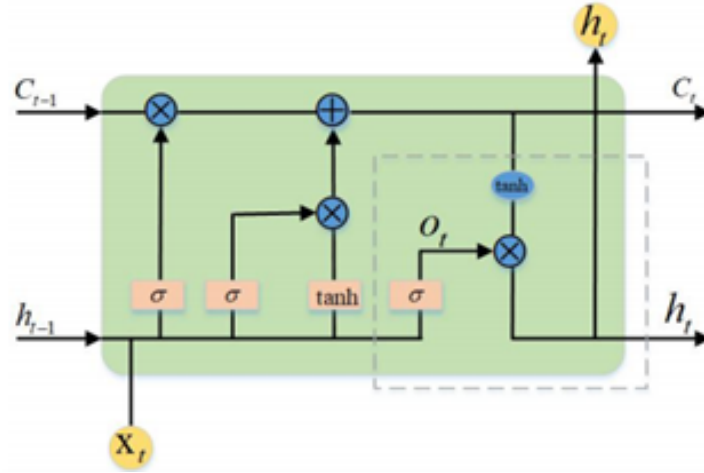


FIGURE 12. Structure of output gate

$$o_t = \sigma(W_o x_t + U_o h_{t-1} + b_o) \quad (6)$$

$$h_t = o_t \circ \tanh(C_t) \quad (7)$$

In the above equations, W_o , and U_o represent the weight matrices that need to be learned through model training for mapping x_t and h_{t-1} to output gate o_t . h_t denotes the current hidden state generated by filtering the squashed cell state $\tanh(C_t)$ through the output gate o_t .

3.2. Data Preprocessing. Data used in this study were extracted from nine road segments at an intersection in the Oakland region of California, USA, in the PeMS system for two months (July–August 2022) of traffic volume data. Data are aggregated at 5-minute intervals, generating a time series of 288 values per day for each roadway segment.

Traffic data collection is a complex process, due to the detection equipment reasons, bad weather, other road conditions, it is inevitable to produce data loss and anomalies and other problems. Whether the data is accurate and effective will directly affect the model's forecasting accuracy. To predict traffic volume more effectively and obtain more accurate prediction results, data preprocessing is necessary for building a short-term traffic volume prediction model using LSTM.

Traffic volume is a time series data that is aggregated at certain time intervals, and there will be a fixed amount of data in a day. Therefore, we can determine whether

there is missing data in a certain time segment by judging the number of data per day or querying the null value. In this paper, the `isnull()` function in Python is used to identify whether there is missing data in the sequence, and if there is missing data, we need to use certain methods to repair it.

Outliers are those data that have very large deviations from other data, such as traffic flow that deviates seriously from road capacity, negative traffic flow, etc. The treatment of outliers in this paper is to first remove them from the dataset and then insert values within the normal variation range at the deleted position.

Considering the computational complexity, this paper adopts the historical mean method for the repair of missing data and anomalous data, the calculation method is shown in (8).

$$\bar{x}_t = \frac{x_{t-1} + x_{t-2} + x_{t-3} + \cdots + x_{t-n}}{n} \quad (8)$$

In (8), \bar{x}_t denotes the calculated average value according to traffic volume data of the previous n moments, n denotes the previous n moments of time t .

Traffic volume has a large amount of variation at different times of the day, so data normalization should be performed before initiating the model training process, with the purpose of unifying the data scale and eliminating the impact of the magnitude difference between the traffic flow feature data on the convergence speed and prediction accuracy of the model [21]. In this paper, the traffic volume data is normalized using the Z-score method, which normalizes the data to zero mean unit variance, and the calculation formula is shown below:

$$x = \frac{X - \mu}{\sigma} \quad (9)$$

In (9), X denotes the traffic volume eigenvalue; μ is the mean value of the eigenvalue of the dataset, σ is the standard deviation of the eigenvalue.

3.3. Traffic Volume Prediction Process Based on LSTM. The forecasting of traffic volume is a time series forecasting task, in the traffic volume prediction using LSTM model, x_t denotes the real value of the traffic volume time series input to the model at time moment t , x_{t+1} denotes the predicted value at time moment $(t + 1)$. During the model training process, the objective function is optimized according to the batch gradient descent algorithm, the objective function is set to MSE. When the training error reaches the minimum or the number of training times reaches a set number of epoch, the training process is stopped to obtain the current prediction value. The following is a description of the specific process of predicting traffic volume using the LSTM model:

- Step 1: Determine the sample length n of the input traffic volume as well as the length of the output data. Use $(x_1, x_2, x_3, \dots, x_n)$ to represent the input traffic volume time series.
- Step 2: Initialize the key parameters for the LSTM model: number of hidden layers, input layer nodes count, hidden layer nodes count and output layer nodes count, etc.
- Step 3: Preprocess the dataset and divide it into training set and prediction set using 80/20 rule.
- Step 4: Train the LSTM network on temporally-ordered data segments generated through sliding window sampling from training set, optimize the objective function and adjust the weights using the batch gradient descent algorithm.
- Step 5: Set different hyperparameters for model training experiments, calculate the predicted values under different hyperparameters, and judge the optimal parameters through evaluation indexes.

- Step 6: After determining each parameter, input the prediction set to the trained model to realize traffic volume forecasting and analyze the results.

3.4. Experiment and Performance Evaluation. In this study, we select road section 3 in Figure 1 as the target section, and extract the traffic volume data of it as the experiment data. Because of the cyclical nature of traffic flow data changes, which changes similarly every week, and the traffic flow trends on weekdays and non-weekdays are significantly different, we train the model and predict using the traffic volumes of weekday and non-weekday separately. For weekday traffic volume prediction, the traffic volume data of weekdays within one month from August 1 to 31, 2022 is selected as the experiment dataset. For traffic flow prediction on non-weekdays, traffic flow data on non-weekdays within two months from July 1 to August 31, 2022 is selected as the experiment dataset to expand the sample size.

3.4.1. Model Evaluation Indicators. We used four common evaluation indicators in this paper to assess the performance of the LSTM-based prediction method, they are MAE, RMSE, MAPE and R^2 . Their calculation formulas are shown in (10)–(13).

$$RMSE = \sqrt{\frac{1}{N} \sum_{i=1}^N (y_i - p_i)^2} \quad (10)$$

$$MAE = \frac{1}{N} \sum_{i=1}^N |y_i - p_i| \quad (11)$$

$$MAPE = \frac{1}{N} \sum_{i=1}^N \frac{|p_i - y_i|}{y_i} \times 100 \quad (12)$$

$$R^2 = 1 - \frac{\sum_{i=1}^N (p_i - y_i)^2}{\sum_{i=1}^N (\bar{y}_i - y_i)^2} \quad (13)$$

In the above three equations, p_i denotes the predicted value of traffic volume at time i , y_i is the observed value of traffic volume, N is the total number of prediction instances, and \bar{y}_i denotes the mean of the observed values.

A strong inverse relationship exists between prediction accuracy and error metrics (RMSE, MAPE and MAE). Higher prediction accuracy is indicated by decreasing RMSE, MAPE and MAE metrics. The greater the R^2 , the more effectively the model explains traffic volume fluctuations [24].

3.4.2. Optimal Parameter Determination and Prediction Performance Analysis. In the LSTM model prediction process, multiple parameters are involved, and whether the parameters are appropriate will to some extent affect the prediction results. These parameters are divided into two categories: one category refers to the parameters that the model continuously adjusts based on the objective function during training, such as weight parameters, and the other refers to the parameters that need to be manually set and adjusted, including the input nodes count, hidden layer nodes count, activation functions, the amount of data processed per batch, learning rates, etc. These parameters are called hyperparameters. There is no fixed method for setting hyperparameters, and most studies use trial and error methods combined with previous research experience to adjust settings based on different data characteristics.

In this experiment, the activation function utilized is sigmoid, and the loss function is MSE. According to several comparison experiments, the model parameters set in this paper are shown in Table 1.

TABLE 1. Key parameter settings for the LSTM-based prediction model

Parameters	For Weekday	For Weekend
Learning rate	0.005	0.0064
Batch size	64	64
Epoch	200	220
Input nodes count	28	20
Hidden layer count	2	2
Hidden nodes count	128	130
Output nodes count	1	1

To validate the effectiveness of the LSTM-based forecasting model, the trained model is employed to forecast traffic volume for both a weekday (August 15, 2022) and a non-weekday (August 28, 2022). Figure 13 presents the forecasting results for weekdays.

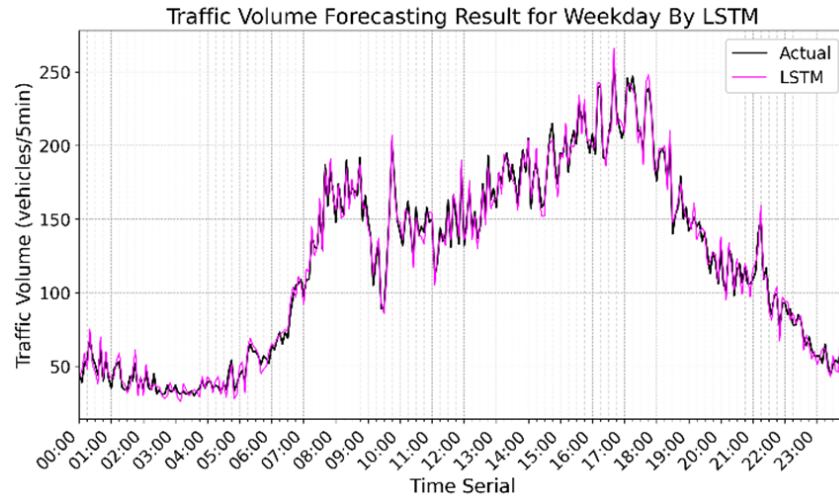


FIGURE 13. Prediction result for weekday

As shown in Figure 13, the LSTM model for weekday traffic volume forecasting capture the general trend of observed traffic volumes, though some discrepancies persist when compared to actual values. The value of RMSE is 10.2951, MAE is 8.0382, MAPE is 6.9778 and R2 is 0.9323.

Figure 14 displays the predicted results for non-weekdays, indicating that the LSTM-based prediction model for non-weekdays predicts a similar trend in traffic volume to the actual traffic volume, but there are still some differences compared to the true traffic volume data. The value of RMSE is 10.0373, MAE is 8.2372, MAPE is 6.6849 and R2 is 0.9369.

4. PG-LSTM Hybrid Prediction Model Integrating Spatial and Temporal Features. As indicated by the preceding feature analysis of traffic volume, it is known that the traffic volume of the current road section in the road network is affected by its own historical data and the surrounding road sections. In order to realize more accurate traffic volume prediction, the model needs to capture two types of features: the historical time

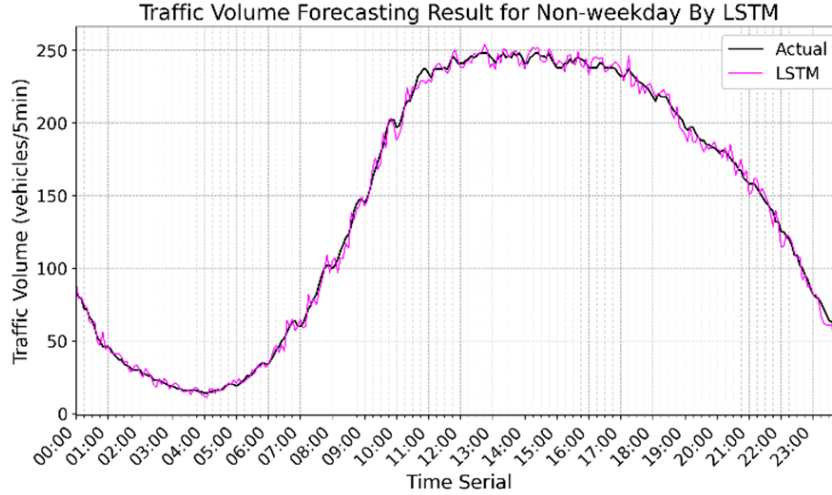


FIGURE 14. Prediction result for non-weekday

series pattern of the target road section itself, and network-wide spatial dependencies with neighboring road sections.

4.1. Modeling of Spatial Feature Analysis. Based on Pearson correlation modeling, the strength of traffic volume correlations between different road segments is assessed, which provides a basis for the extraction of traffic volume spatial features. According to the analysis of the spatial correlation of 9 road segments shown in Figure 8, target road segments 1, 3, 4, 6, 8 and 9 with high correlation over 0.90 are selected for spatial feature modeling.

4.2. Spatial Feature Modeling. Accurate capture of spatial correlations in traffic networks is a critical issue in spatial features modeling. CNN has developed earlier and can handle local network structures well. It is mainly used in Euclidean space and has significant advantages in image recognition processing. However, road networks only have graphical forms, not real images, so CNN models cannot reflect the structural characteristics of road networks, let alone effectively extract their spatial dependencies. In recent years, GCN breaks the limitation that CNN only deals with grid-structured data, and successfully extends CNN to the graph domain space, which shows obvious advantages in modeling complex graph structures, and has already achieved success in the fields of social network analysis, knowledge graph, and recommender system. In this study, we utilize GCN to capture and represent the spatial features of traffic volume across multiple selected road segments.

The road network can be described as an unweighted and undirected graph structure, and represented by graph $G = (V, E)$. Taking each road segment as a vertex v , the vertex set can be expressed as $V = \{v_1, v_2, \dots, v_N\}$, here N denotes the count of vertices. E denotes the edge set which captures and represents all direct linkage relationships between the graph nodes. The graph's connectivity structure is represented as adjacency matrix A , which only contains elements 0 and 1. If there is no connection between two roads, it is represented as 0, and if there is a connection, it is represented as 1.

In the GCN framework, we define the road network's traffic volume data as node attributes $X \in \mathbb{R}^{N \times P}$, where P denotes the dimension of feature vectors corresponding to the length of historical observations. The traffic state at time interval t is represented by $X_t \in \mathbb{R}^{N \times t}$. The traffic volume forecasting task integrating spatiotemporal features can thus be formulated as:

$$[X_{t+1}, \dots, X_{t+T}] = f(G : (X_{t-n}, \dots, X_{t-1}, X_t)) \quad (14)$$

In (14), n denotes the count of time points in the input sequence i.e. length of the input sequence, T specifies the count of future time points to be predicted i.e. length of the output sequence, and f denotes the mapping function to be learned through model training.

Given adjacency matrix A and node feature matrix X , the GCN initially normalizes the graph structure, then applies learnable parameter matrices to linearly transform the aggregated neighborhood features. Coupled with nonlinear activation functions, it achieves hierarchical feature propagation, thereby capturing both local and global spatial dependencies in traffic networks, ultimately extracting spatial-aware features for prediction tasks [25], which can be expressed as the following equation.

$$H^{(L+1)} = \sigma(\tilde{D}^{-1/2} \hat{A} \tilde{D}^{-1/2} H^{(L)} \theta^{(L)}) \quad (15)$$

The matrix $\hat{A} = A + I_N$ is obtained by adding the identity matrix I_N to A , and \tilde{D} denotes the corresponding degree matrix, $\tilde{D}_{ii} = \sum_j \hat{A}_{ij}$. The degree matrix \tilde{D} is a diagonal matrix where each diagonal entry \tilde{D}_{ii} corresponds to the degree of vertex i , and the degree of the vertex represents the number of sections connected to the vertex. $H^{(L)}$ denotes the node feature matrix of layer L , initially $H^{(0)}$ is E . $\theta^{(L)}$ comprises the model parameters of layer L , which is centered on a series of optimizable weight matrices. σ denotes the activation function. This study employs a single-layer GCN to model spatial correlations in traffic volume patterns, as formulated by the following equation:

$$f(X, A) = \sigma(\tilde{A} X W_0) \quad (16)$$

$$\tilde{A} = \tilde{D}^{-1/2} \hat{A} \tilde{D}^{-1/2} \quad (17)$$

In the above formulas, \tilde{A} represents the pre-processing process, which aims to balance the influence of node degree and avoid nodes with high degree dominating feature propagation. $W_0 \in \mathbb{R}^{P \times H}$ denotes the learnable projection matrix transforming input features X to hidden state. P is dimension of input feature vectors. H is the number of nodes in the hidden layer [26]. The activation function σ throughout this study is the ReLU function. The output $f(X, A) \in \mathbb{R}^{N \times H}$ represents the traffic flow features of each node (road segment) in the road network after aggregating the spatial neighborhood information, which will be fed into the LSTM module for the next prediction.

4.3. The PG-LSTM Prediction Model.

4.3.1. Overall Structure of PG-LSTM Model. The PG-LSTM model is structurally divided into three modules: a Pearson correlation coefficient calculator, a graph convolutional network (GCN) layer, a long short-term memory (LSTM) module. Firstly, the Pearson correlation coefficient method is utilized to screen out the road segments with high spatial correlation to target road segment as the basis for constructing the network topology. Then, using traffic volume feature matrices and adjacency matrices of selected road segments as inputs, the GCN is employed to extract topological relationships within the road network to learn spatially-correlated feature representations. Finally, the traffic volume time series that integrates spatial features are used as input for the LSTM module to capture the temporal features and obtain the final prediction results. The specific calculation formula is as following (18)–(23).

$$i_t = \sigma(W_i[f(A, X_t), h_{t-1}]) + W_i h_{t-1} + b_i \quad (18)$$

$$\tilde{C}_t = \sigma(W_c[f(A, X_t), h_{t-1}]) + W_c h_{t-1} + b_c \quad (19)$$

$$F_T = \sum (W_F[F(A, X_T), H_{T-1}]) + W_F H_{T-1} + B_F \quad (20)$$

$$o_t = \sigma(W_o[f(A, X_t), h_{t-1}]) + W_o h_{t-1} + x_t b_o \quad (21)$$

$$C_t = f_t \circ C_{t-1} + i_t \circ \tilde{C}_t \quad (22)$$

$$h_t = o_t \circ \tanh(C_t) \quad (23)$$

Where w is the weight that needs to be adjusted for optimization during the training process and b is the bias term. The final predictions are generated by propagating the features through a fully connected output layer. The structure of the PG-LSTM model is shown in Figure 15.

4.3.2. Prediction Process Based on PG-LSTM Model. The working mechanism of the PG-LSTM model encompasses the following critical steps:

Step 1: First, calculate the Pearson correlation coefficients between roadway segments according to the traffic volume time series, and select the most highly correlated road segments with target road segment based on certain correlation coefficient thresholds, the threshold in this study is 0.90.

Step 2: Preprocess the data to form a weekday dataset and a non-weekday dataset, and then divide each dataset into two parts, one for model training and one for model testing.

Step 3: Train the model on the training set. Employ a GCN consisting of a single convolutional layer and pooling layer to extract topological relationships within the road network and learn spatially relevant feature representations. The input consists of the standardized traffic volume dataset and the adjacency matrix, and the output is the traffic volume features fused with spatial features.

Step 4: The output of the GCN is fed into the LSTM module to capture the temporal dependencies in traffic volume. The output of LSTM module represents a forecast of the traffic volume for the subsequent time interval.

Step 5: The model's final output data must be denormalized to restore the original scale and obtain the final prediction results.

4.3.3. Experiment and Performance Evaluation. This paper uses RMSE, MAE, MAPE and R2 as evaluation indicators for the forecast results generated by the PG-LSTM model.

The PG-LSTM model's performance is influenced by some hyperparameters, such as the learning rate, training iterations (epochs), batch size, hidden unit quantity and so on. The setting of some parameters refer to the method of LSTM prediction model in the previous section. The length of the history sequence of node traffic volume features and the hidden node quantity are very important parameters in the PG-LSTM model, and different lengths of the history sequence and hidden node quantity will significantly influence the prediction accuracy. This study employs comparative experiments method to select more appropriate parameter values, and after several experiments, the model parameters were selected finally as shown in Table 2.

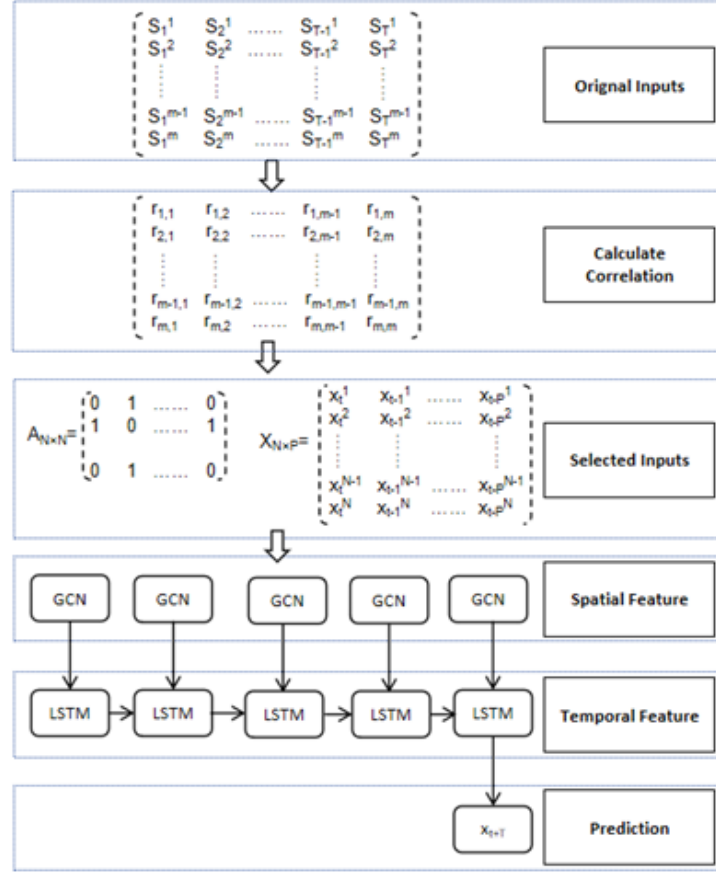


FIGURE 15. Overall Structure of PG-LSTM model

TABLE 2. Key parameter settings for the PG-LSTM model

Parameters	For Weekday	For Weekend
Learning rate	0.001	0.0012
Batch size	64	32
Epoch	300	240
Sequence length	16	12
Hidden nodes count for GCN	32	32
Input nodes count for LSTM	32	32
Hidden nodes count for LSTM	128	130
Loss function	MSE	MSE

To assess the predictive capability of the PG-LSTM prediction model, we utilized the trained model to predict traffic volume on both a weekday (August 15, 2022) and non-weekday (August 28, 2022) scenario. Figure 16 displays the predicted results for weekdays, Figure 17 displays the predicted results for non-weekdays.

From Figure 16 and Figure 17, it can be seen that the prediction results of the PG-LSTM model are better fitted to the actual trend of the traffic volume.

In order to further analyze the forecasting performance of the PG-LSTM model, four other models (CNN-LSTM, LSTM, BP and GRU) are used to forecast the traffic flow on the same road section. The weekday traffic forecasting results are visualized in Figure 18, while those for the non-weekday are presented in Figure 19.

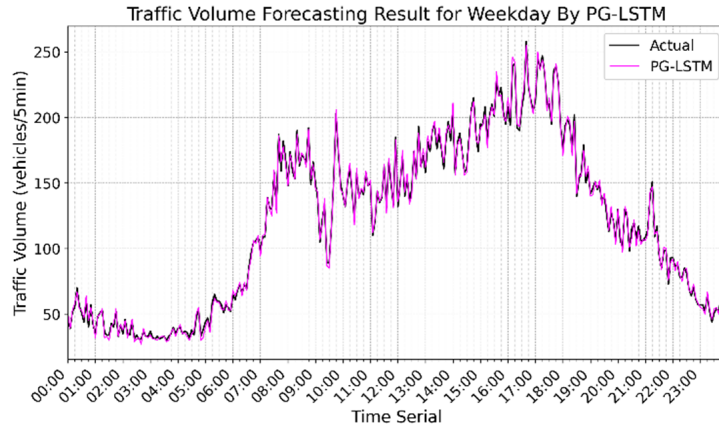


FIGURE 16. Prediction result of PG-LSTM model for weekday traffic volume

FIGURE 17. Prediction result of PG-LSTM model for non-weekday traffic volume

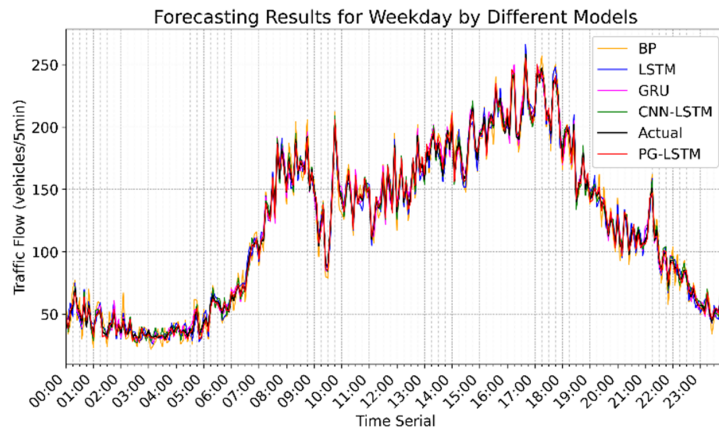


FIGURE 18. Prediction result of PG-LSTM and reference models for weekday traffic volume

Table 3 and Table 4 comparatively present the traffic volume prediction performance of the proposed PG-LSTM hybrid model against other methods (CNN-LSTM, LSTM, GRU, and BP) for weekday and weekend scenarios, respectively.

TABLE 3. The evaluation results of distinct models for weekday traffic volume forecasting

Models	RMSE	MAE	MAPE	R2
PG-LSTM	7.6102	6.4025	4.7042	0.9768
CNN-LSTM	8.9203	7.0415	5.8725	0.9584
LSTM	10.2951	8.0382	6.9778	0.9323
GRU	10.1128	8.1046	7.1269	0.9306
BP	14.2064	11.4218	10.1802	0.8976

The comparative analysis of prediction performance demonstrates that the proposed PG-LSTM model achieves significantly lower prediction errors than the CNN-LSTM and

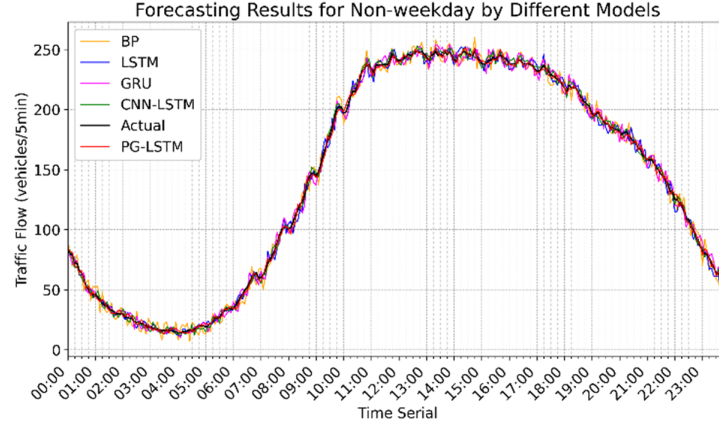


FIGURE 19. Prediction result of PG-LSTM and reference models for non-weekday traffic volume

TABLE 4. The performance evaluation results of different models for traffic volume forecasting on non-weekdays

Models	RMSE	MAE	MAPE	R2
PG-LSTM	7.0235	6.2061	4.5485	0.9773
CNN-LSTM	8.2027	7.2303	5.4778	0.9602
LSTM	10.0373	8.2372	6.6849	0.9369
GRU	10.4103	8.2014	6.7598	0.9251
BP	14.8106	11.1038	9.9781	0.8901

other baseline models. This indicates that the PG-LSTM hybrid model, by effectively extracting and integrating spatial-temporal features of traffic volume, can predict short-term traffic volume data with greater accuracy. With the R^2 value exceeding 0.97, the model exhibits strong explanatory power for traffic volume dynamics.

5. Conclusion. The study utilizes actual traffic volume records collected from an intersection in the Oakland area of California, USA, in the PeMS system. Firstly, it analyzes the temporal and spatial features of the traffic volume. The temporal feature analysis reveals that the traffic volume data changes show periodicity. The traffic volume change trends on weekdays within a week are similar, and the intra-day change trends of the same weekday in different weeks are basically the same. The intra-day traffic volume changes on non-weekdays present different characteristics from those on weekdays. Spatial feature analysis indicates that traffic volumes among different sections of the transportation network have mutual influences, especially the traffic volume changes between adjacent sections are closely related. The calculation of Pearson correlation coefficient quantitatively proves the above conclusion. Then the LSTM-based traffic forecasting model is constructed to perform traffic volume forecasting for individual road sections, and the experiments show that the LSTM can effectively capture the temporal features of the traffic volume. In order to further improve the accuracy of traffic volume prediction, spatial correlations in traffic data must be accounted for predictive modeling. To address this, we propose an integrated traffic volume prediction model named PG-LSTM by combining PCC, GCN and LSTM: Firstly, the traffic volume correlation coefficients between different road sections in the traffic network are calculated, and highly correlated road sections are selected based on their correlation coefficients with the target segment. Then by formulating the traffic network as a graph structure with road segments as nodal

elements, we subsequently develop a GCN framework to extract spatial dependencies in traffic volume. Finally, propagates the GCN-generated traffic features integrating spatial dependencies into the LSTM module, so as to effectively combine spatial and temporal patterns for traffic prediction. Experimental comparisons with CNN-LSTM, LSTM, GRU, and BP models demonstrate that PG-LSTM achieves significant advantages over all evaluation metrics (RMSE, MAE, MAPE and R^2). The results confirm PG-LSTM's enhanced capability in jointly modeling spatiotemporal traffic volume patterns.

Acknowledgment. This work was funded by the Anhui Provincial Natural Science Project KJ2019A0878, the National First-level Professional Construction Project 2020ylzy01, and the Anhui Provincial Traditional Professional Enhancement Project 2023zygzts105.

REFERENCES

- [1] J. F. Wang, H. P. Lu, H. Peng, "System dynamics model of urban transportation system and its application," *Journal of Transportation Systems Engineering and Information Technology*, vol. 8, no. 3, pp. 83–89, Mar. 2008.
- [2] M. Lippi, M. Bertini, P. Frasconi, "Short-term traffic flow forecasting: An experimental comparison of time-series analysis and supervised learning," *IEEE Trans. Intell. Transp. Syst.*, vol. 14, no. 2, pp. 871–882, Jun. 2013.
- [3] E. I. Vlahogianni, M. G. Karlaftis, J. C. Golias, "Short-term traffic forecasting: where we are and where we're going," *Transportation Research Part C: Emerging Technologies*, vol. 43, no. 1, pp. 3–19, Jun. 2014.
- [4] I. Okutani, Y. J. Stephanedes, "Dynamic prediction of traffic volume through Kalman filtering theory," *Transportation Research Part B: Methodological*, vol. 18, no. 1, pp. 1–11, 1984.
- [5] Z. Liu, X. Qin, W. Huang, X. Zhu, Y. Wei, J. Cao, et al., "Effect of Time Intervals on K-nearest Neighbors Model for Short-term Traffic Flow Prediction," *Promet - Traffic & Transportation*, vol. 31, no. 2, pp. 129–139, 2019.
- [6] G. K. Shen, "Short-term Traffic Flow Prediction Based on Harmony Search Algorithm Optimized Wavelet Neural Network," *J. Phys.: Conf. Ser.*, vol. 1682, 2020.
- [7] R. Tang, Q. C. Chen, X. F. Lei, "GQPSO-WNN Short-Term Traffic Flow Prediction Based on Phase Space Reconstruction," *Computer Applications and Software*, vol. 36, no. 07, pp. 311–316, 2019.
- [8] Y. Zhang, G. Huang, "Traffic flow prediction model based on deep belief network and genetic algorithm," *IET Intelligent Transport Systems*, vol. 12, no. 6, pp. 533–541, 2018.
- [9] Y. Jin, W. Xu, P. Wang, and J. Yan, "SAE Network: A deep learning method for traffic flow prediction," in *Proc. 5th Int. Conf. Inf., Cybern., Comput. Social Syst. (ICCSS)*, 2018.
- [10] R. Soua, A. Koesdwiady, and F. Karray, "Big-data-generated traffic flow prediction using deep learning and Dempster-Shafer theory," in *Proc. IJCNN*, 2016.
- [11] R. Madan, P. Sarathimangipudi, "Predicting computer network traffic: A time series forecasting approach using DWT, ARIMA and RNN," *IEEE Access*, vol. 6, pp. 1–5, 2018.
- [12] Y. Kim, P. Wang, L. Mihaylova, "Scalable Learning with a Structural Recurrent Neural Network for Short-Term Traffic Prediction," *IEEE Sensors Journal*, vol. 19, no. 23, pp. 11359–11366, 2019.
- [13] W. Zhang, Y. Yu, Y. Qi, F. Shu, Y. Wang, "Short-term traffic flow prediction based on spatio-temporal analysis and CNN deep learning," *Transportmetrica*, vol. 15, no. 2, pp. 1688–1711, 2019.
- [14] H. Yu, Z. Wu, S. Wang, Y. Wang, X. Ma, "Spatiotemporal Recurrent Convolutional Networks for Traffic Prediction in Transportation Networks," *Sensors*, vol. 17, no. 7, Jul. 2017, Art. no. 1501.
- [15] Z. R. Ge, S. Dai, "A Spatio-temporal Traffic Flow Forecasting Method Based on WAC-GCN," *Academic Journal of Computing & Information Science*, vol. 7, no. 5, pp. 87–93, 2024.
- [16] H. Zhang, G. Yang, H. L. Yu, Z. Zheng, "Traffic flow prediction based on the RETGCN model," *Computing*, vol. 107, no. 1, pp. 49–59, 2025.
- [17] L. Kang, G. Hu, H. Huang, W. Lu, L. Liu, "Urban traffic travel time short-term prediction model based on spatio-temporal feature extraction," *Journal of Advanced Transportation*, vol. 2020, no. 332, pp. 1–16, Aug. 2020.
- [18] D. Pavlyuk, "Feature selection and extraction in spatiotemporal traffic forecasting: A systematic literature review," *European Transport Research Review*, vol. 11, no. 1, pp. 6–23, Dec. 2019.

- [19] C. F. Shao, S. Xue, C. J. Dong, S. Y. Wang, Y. Zhuang, "Short-term network traffic flow prediction considering spatiotemporal correlations," *Journal of Beijing Jiaotong University*, vol. 45, no. 1, pp. 1–9, 2021.
- [20] R. T. Vollmer, "Multivariate statistical analysis for pathologist. part i, the logistic model," *American Journal of Clinical Pathology*, vol. 105, no. 1, pp. 115–126, Jan. 2016.
- [21] J. D. Wang, C. O. N. Susanto, "Traffic flow prediction with heterogenous data using a hybrid cnn-lstm model," *Computers, Materials & Continua*, vol. 76, no. 3, pp. 2801–2816, 2023.
- [22] S. Y. Ma, M. Zhao, "Traffic flow prediction and analysis in smart cities based on the WND-LSTM model," *Computational Intelligence and Neuroscience*, vol. 2022, no. 1, pp. 1–15, Aug. 2022.
- [23] H. Y. Wen, D. R. Zhang, "Expressway traffic volume prediction based on Bi-LSTM model," *Highway Eng.*, vol. 44, no. 6, pp. 6–12, 2019.
- [24] A. A. Kashyap, S. Raviraj, A. Devarakonda, S. R. Nayak, S. K. V., and S. J. Bhat, "Traffic flow prediction models – A review of deep learning techniques," *Cogent Eng.*, vol. 9, no. 1, p. 2010510, Dec. 31 2022.
- [25] P. Liu, Y. Xu, J. Ma, J. Liang, H. Xiao, and Y. Cong, "Multi-radar collaborative networking method based on T-GCN," *Journal of Physics: Conference Series*, vol. 1976, no. 1, p. 012037, 2021.
- [26] L. Zhao, Y. Song, C. Zhang, Y. Liu, H. Li, "T-GCN: a temporal graph convolutional network for traffic prediction," *IEEE Trans. Intell. Transp. Syst.*, vol. 21, no. 9, pp. 3848–3858, Sept. 2020.